ASSESSMENT OF GLOBAL AND LOCAL PRESSURE WAVE REFLECTION IN THE AORTA OF PATIENTS WITH MARFAN DISEASE

P. Segers[*], J. De Backer[**], D. Devos[**], S.I. Rabben[***], T.C. Gillebert[**], L.M. Van Bortel[**], J. De Sutter[**], A. De Paepe[**], P.R. Verdonck[*]

[*]Cardiovascular Mechanics and Biofluid Dynamics, Ghent University, Gent, Belgium
[**]Ghent University Hospital, Gent, Belgium
[***]Institute for Surgical Research, Rikshospitalet University Hospital, Oslo, Norway

patrick.segers@ugent.be

Abstract: Central pressure and flow waveforms were assessed in 26 patients with Marfan syndrome (MFS; age 13-54 yrs) and in 26 age and sex matched controls (CTRL) using ultrasound and magnetic resonance imaging. Calculated *global* wave reflection indices were the augmentation index (AIx) and the ratio of backward-to-forward pressure wave (P_b/P_f). In addition, systolic and diastolic cross-sectional area of the aorta was measured at 4 levels: ascending (AA) and descending (DA) aorta, diaphragm (DIA) and low abdominal aorta (AB). From these, local characteristic impedance was calculated as well as *local* reflection coefficients ($\Gamma_{xx\text{-}yy}$) from differences in characteristic impedance. Data were analyzed with age categorized in tertiles using covariance techniques. AIx was higher in MFS than in CTRL, but the difference was significant in the first tertile only (104.9±3.6 % versus 90.4±3.4 %, P<0.05). Similar observations applied to P_b/P_f, but differences did not reach statistical significance (0.52±0.03 versus 0.43±0.03, P=0.12). In CTRL, $\Gamma_{AA\text{-}DA}$ significantly decreased with age (r=-0.55; P<0.01). $\Gamma_{DIA\text{-}AB}$, in contrast, increased with age (r=0.59; P<0.01). In MFS, no correlation with age was found in any segment. We conclude that both global and local wave reflection characteristics are altered in Marfan disease.

Introduction

The Marfan syndrome (MFS) is a genetic connective tissue disorder with manifestations in different organ systems (a.o. ocular and skeletal) and also affecting the aorta [1,[2,[3,[4]. One of the manifestations of the disease is dilatation of the proximal part of the aorta. With the increase in vessel diameter (leading to higher wall stress) and the structural impairment of the vessel, the artery is at an increased risk of dissection and vessel rupture. As such, it is important to recognize all factors that may contribute to an increased load on the aorta in these patients.

It is generally accepted that the early return of reflected pressure waves leads to an increase in central systolic and pulse pressure [5], and may hence contribute to an increased load. This may particularly be true for patients with Marfan disease, where different aspects of the disease should contribute to alterations of arterial wave reflection. Elevated aortic pulse wave velocity due to global aortic stiffening [4,[6,[7] has been reported in these patients, which would favour the early return of pressure waves from the periphery. The disease also primarily affects the proximal part of the aorta, and may change the gradual proximal-to-distal evolution of the mechanical properties of the aorta and give rise to reflections arising from impedance mismatch along the aorta. None of these aspects have been studied before.

The aim of this study was therefore to assess wave reflection in patients with Marfan disease using both global wave reflection indices (such as the augmentation index or the global reflection coefficient), as well as local aortic reflection due to local changes in characteristic impedance.

Materials and Methods

The population studied consisted of twenty-six patients with confirmed MFS (age range 13-54 yrs) and 26 age and sex matched control subjects (CTRL) (see also Table 1). All subjects underwent a 1-day measurement protocol including echocardiography and magnetic resonance imaging (MRI) for the assessment central pressure and flow waveforms and systolic and diastolic dimensions of the aorta at different levels.

Assessing central pressure waveforms (P_{ao})

Central pressure waveforms were obtained via calibration of carotid diameter distension waveforms [8]. With the subject in supine position, a sequence of carotid artery diameter distension tracings typically containing 3 to 5 complexes was measured with a commercially available ultrasonographic system (Vivid 7, GE Vingmed Ultrasound, Horten, Norway) and a 12 MHz vascular probe (12L). The tracing was averaged to obtain one representative waveform which was subsequently transformed into a carotid pressure waveform [9] which is further used as a surrogate of the central pressure waveform (P_{ao}). To do so, it was assumed that the relation between pressure and diameter was linear, and that diastolic (DBP) and mean arterial pressure (MAP) was similar at the brachial and carotid artery. MAP was assessed following a procedure as

ISSN: 1727-1983

recently described by Verbeke et al. [10]. Central systolic blood pressure (SBP) was taken as the maximum value of P_{ao}.

Assessing central flow waveforms (Q_{ao})

Blood flow velocities were acquired in the left ventricular outflow tract (LVOT) using pulsed wave Doppler (3.5 MHz probe) in the apical 5-chamber view, stored as DICOM images and contours were semi-automatically traced with a dedicated software interface written in Matlab (The Mathworks, Natick, Massachusetts). An ensemble average was constructed of minimally three cycles, and the average curve was scaled so that the area under the curve matched stroke volume (SV) as determined from MRI (see further for a description of the MRI protocol). We judged this approach to be the most accurate because LVOT diameters were difficult to assess accurately in Marfan patients with dilated aortic roots. The aortic flow waveform is further indicated as Q_{ao}. Cardiac output (CO) was obtained as the product of SV and heart rate (HR). It was verified that heart rate was similar (+/-5 beats/min) during MRI and ultrasound measurements, which was the case in all subjects.

Global wave reflection: AIx and P_b/P_f

Global wave reflection was, on one hand, quantified using the augmentation index (AIx), calculated as

$$AIx = 100\frac{P_2 - DBP}{P_1 - DBP} \tag{1}$$

P_1 and P_2 are either SBP, either the pressure associated with an inflection point visually identified on P_{ao} (see also Figure 1). The pressure occurring first is labeled as P_1. AIx formally quantifies the pressure waveform classification scheme as first described by Murgo et al. [11,[12] AIx<100% indicates arrival of the pressure wave in late systole; AIx > 100% is indicative for arrival in early systole.

As demonstrated by Westerhof et al. [13], the pressure wave is composed of a forward (P_f) and a reflected or backward (P_b) travelling component, which can be separated from each other provided that P_{ao} and Q_{ao} are known, as well as characteristic impedance (Z_0):

$$P_f = \frac{(P_{ao} + Z_0 Q_{ao})}{2}; P_b = \frac{(P_{ao} - Z_0 Q_{ao})}{2} \tag{2}$$

One can then define the global wave reflection coefficient as the ratio of the amplitudes of P_b and P_f (P_b/P_f).

Z_0 was estimated as the average value of the modulus of the high frequency components of input impedance [14,[15].

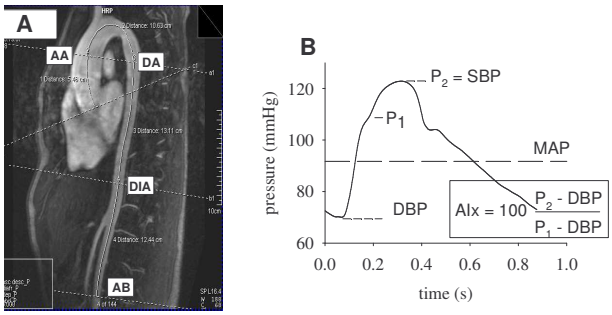

Figure 1. Panel A: MRI angiography with indication of the 4 measurement levels along the aorta. Panel B: calibrated carotid distension wave (P_{ao}) and indication of diastolic (DBP), mean (MAP) and systolic (SBP) blood pressure, as well as P_1 (inflection point) and P_2 for the calculation of AIx.

MRI: stroke volume and aortic dimensions.

All subjects were scanned on a 1.5T MR system (Magnetom Symphony, Siemens, Erlangen, Germany) with ECG gating. Left ventricular volumes were acquired with an ECG triggered trueFISP (Fast Imaging with Steady-state Precession) sequence and SV was calculated as the difference between end-diastolic and end-systolic volume.

Aortic systolic (A_{xxs}) and end-diastolic (A_{xxd}) cross-sectional area was measured using trueFISP images (temporal resolution of 25 milliseconds) obtained at 4 levels (indicated by xx) along the aorta: the ascending (AA) and descending thoracic aorta (DA), thoracic-abdominal aorta near the diaphragm (DIA) and low abdominal aorta (AB) (see Figure 1).

Local wave reflection: Γ

Local reflection, arising from impedance mismatch between levels xx and yy, was quantified using local wave reflection coefficients ($\Gamma_{xx\text{-}yy}$) calculated as

$$\Gamma_{xx-yy} = \frac{Z_{0-yy} - Z_{0-xx}}{Z_{0-yy} + Z_{0-xx}} \tag{3}$$

where $Z_{0\text{-}xx}$ is the characteristic impedance at level xx, approximated as

$$Z_{0-xx} = \sqrt{\frac{\rho}{A_{xx}}\left(\frac{SBP - DBP}{A_{xxs} - A_{xxd}}\right)} \tag{4}$$

with ρ the density of blood (assumed 1030 kg/m^3) and A_{xx} the average value of A_{xxs} and A_{xxd}.

Statistical analysis

All reported data are mean ± standard errors on the mean. Population means were compared using Student's t-test. Data were organized in tertiles of age (≤27 years, >27 and ≤ 40 years, > 40 years) and analyzed using covariance techniques. Relation between parameters was studied using Pearson correlation and linear

ISSN: 1727-1983

regression analysis. All analysis was performed in SPSS (Version 11.5, SPSS Inc., Chicago, Illinois).

Results

Marfan subjects were taller, had a higher weight and body surface area (BSA) than controls (Table 1). There was no difference between MFS and CTRL for age, body mass index, brachial and central blood pressure, heart rate (HR), stroke volume and cardiac output. General hemodynamic data and patient characteristics are summarized in Table 1.

Table 1. Population characteristics and general hemodynamic data. Data are mean values ± standard error on the mean. P-values: CTRL vs. MFS (t-test).

	CTRL (n=26)	MFS (n=26)	P-value
M/F	12/14	12/14	1.00
Age (years)	35.9 ± 2.3	32.7 ± 2.2	0.33
Length (m)	1.73 ± 0.02	1.83 ± 0.02	0.0009
Weight (kg)	67.0 ± 2.6	75.4 ± 2.8	0.03
BSA (m^2)	1.80 ± 0.04	1.98 ± 0.04	0.003
DBP (mmHg)	62.7 ± 1.7	61.1 ± 1.8	0.53
MAP (mmHg)	84.4 ± 1.9	83.2 ± 1.7	0.65
SBP (mmHg)	104.8 ± 2.4	106.4 ± 2.3	0.64
HR (beats/min)	67.0 ± 2.0	61.8 ± 2.0	0.07
SV (ml)	78.9 ± 4.6	82.0 ± 5.5	0.67
CO (l/min)	5.2 ± 0.2	4.9 ± 0.3	0.51

Mean age within each tertile was 22.9 ± 1.0 (N = 20; 9 controls), 33.8 ± 1.1 (N = 16; 9 controls) and 48.4 ± 1.4 year (N = 16; 8 controls). Augmentation index, AIx, was 102.1 ± 3.1% in CTRL versus 103.3 ± 2.1 % in MFS, a difference which was not significant in t-test analysis (P=0.75). Interestingly, analysis of covariance adjusting for length increased the average difference between both groups (99.9 ± 2.2 % in CTRL versus 105.7 ± 2.1 % in MFS; P=0.19). AIx increased less with age in MFS than in CTRL (P<0.05), but it was significantly higher (104.9 ± 3.6 % versus 90.4 ± 3.4 %; P<0.05) in MFS in the first age tertile (Figure 2, panel A).

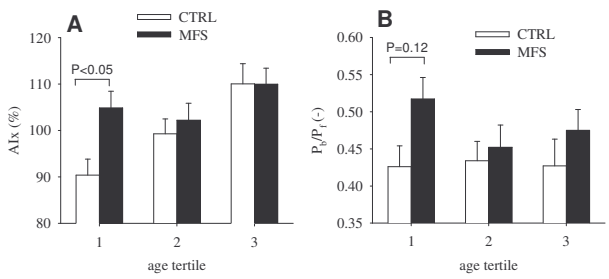

Figure 2: Panel A: variation of the augmentation index, AIx, with age (per tertile); panel B: variation of P_b/P_f with age. Displayed values are adjusted for body size. Error bars represent standard errors on the mean.

Similar to AIx, there was no difference in P_b/P_f between patients with Marfan syndrome (0.47 ± 0.02) and controls (0.45 ± 0.02; P=0.44) in t-test analysis. Covariance analysis, with length designated as the only significant covariant, demonstrated a tendency for higher P_b/P_f in MFS (P=0.053), with length-adjusted P_b/P_f estimated to be 0.48 ± 0.02 in MFS versus 0.43 ± 0.02 in CTRL. Length-corrected values for P_b/P_f per tertile are given in Figure 2 (panel B). The difference was again most outspoken in the youngest group, but did not reach statistical significance (0.52 ± 0.03 versus 0.43 ± 0.03, P=0.12).

Local reflection coefficients are displayed in Figure 3 as a function of location and age (tertile). In CTRL, $\Gamma_{AA\text{-}DA}$ (proximal aorta) progressively decreased with age (P<0.05), while $\Gamma_{DIA\text{-}AB}$ (distal aorta) increased with age (P<0.05). Statistically significant age-related changes in local reflection coefficients were absent in MFS. Comparing MFS to CTRL, $\Gamma_{AA\text{-}DA}$ was overall lower in MFS than in CTRL (P<0.05). The difference was significant in tertile 2 (P<0.05). There was a trend towards a higher $\Gamma_{DIA\text{-}AB}$ in CTRL in tertile 3 (P = 0.12).

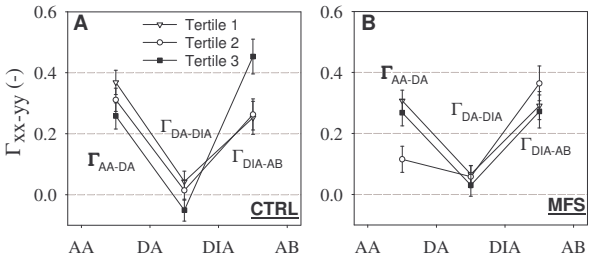

Figure 3. Variation of local reflection coefficients ($\Gamma_{xx\text{-}yy}$) along the aorta (AA: ascending aorta; DA: descending aorta; DIA: diaphragm; AB: lower abdominal aorta) in controls (panel A) and Marfan patients (panel B). Data are grouped per tertile of age; error bars are standard errors on the mean.

Discussion

Our results indicate that arterial wave reflection is altered in patients with Marfan disease, both at a global and local level. When compared with age and sex-matched controls, AIx is higher in Marfans, a difference that is particularly pronounced in young adults. As for the local reflection properties of the aorta, control subjects showed an age related decrease in proximal reflection coefficient and a progressive increase in distal reflection coefficient. In contrast, Marfan patients exhibited no significant changes with age in local reflection coefficients.

Wave reflections are generated by mismatches in characteristic impedance, the latter being determined by the stiffness of the vessel, and its calibre [14,[15]. It is generally accepted that in the normal population, there is a gradual increase in impedance along the aorta (due to geometric and elastic taper [16]) but that impedance mismatch is most important in the periphery, where small-sized arteries make the transition to arterioles and

ISSN: 1727-1983

capillaries. In the control population in this study (Figure 3, panel A), we found positive local reflection coefficients (order of magnitude 0.3) in the proximal and most distal part of the aorta, with a virtual absence of local reflection in the middle part. $\Gamma_{AA\text{-}DA}$ progressively decreased with age as the impedance of the proximal aorta increases (arterial stiffening), and the impedance difference with the adjacent distal aortic section diminishes. As for the distal part, $\Gamma_{DIA\text{-}AB}$ increased with age due to the more rapid increase in impedance in the most distal part of the aorta. For the control group, we can confront our results with literature findings. Ting et al. reported that local wave reflection can differ remarkably along different regions in the aorta, with pronounced reflections in the ascending aorta and from just proximal to the renal arteries to the aorto-iliac bifurcation, but not in the mid thoracic region [17]. This is in full accordance with our data (Figure 3). More rapid mechanical aging (in the normal population) near the aortic bifurcation has been reported by Gillesen et al [18].

It is well documented that the most prominent manifestation of Marfan disease at the level of the blood vessels is dilatation of the aortic root and the proximal part of the aorta and an increase in vessel stiffness and pulse wave velocity [3,[4,[6]. It is, however, unknown whether these mechanical alterations favour the generation of reflected waves at locations close to the heart, potentially increasing the load on central arteries. Our data (Figure 3) suggest that this is not the case, at least not along the aorta. If any effect is noticed, the local alterations at the proximal aorta rather diminish the impedance differences between adjacent aortic sections, reducing the local reflection coefficients instead of increasing them. Note, however, that our data only cover the aorta itself, and do not provide any information on the impedance difference between the aorta and large arteries branching off the aorta.

Despite the absence of clear differences between MFS and CTRL in the absolute values of the local reflection coefficients along the aorta, there were marked differences between the studied groups in the evolution of Γ with age. While there were clear and explicable trends in the data for the control group, these were absent for the Marfan patients. The overall lower value of $\Gamma_{AA\text{-}DA}$ in MFS points in the direction of "more rapid aging" of the proximal aorta in MFS, which is in agreement with biomechanical observation and histo-pathological findings. We speculate that inter-patient differences in severity of the disease complicate the detection of eventual age-related patterns in this patient group.

In addition to local aortic reflection properties, we also studied global indices of wave reflection, such as the augmentation index and the global wave reflection coefficient. Here, we did find significant differences between CTRL and MFS, an observation that was earlier made by Yin et al. [19]. Analysis of covariance, correcting for differences in stature between the two populations, indicated an elevated AIx and P_b/P_f, with differences reaching (AIx) or approaching (P_b/P_f) statistical significance in the youngest subgroup (tertile 1). AIx is an integrated index, affected by all parameters influencing timing (path length, pulse wave velocity, location of reflection points, heart rate) and magnitude (P_b/P_f) of the reflected waves. Aortic pulse wave velocity is generally increased in MFS [6], which certainly partly explains the higher AIx in this patient group. As a first analysis, we calculated the correlation coefficients between AIx, P_b/P_f and the local reflection coefficients (Table 2). It can be noticed that P_b/P_f shows a reasonable correlation with AIx, and it can be expected that the higher AIx in tertile 1 is also driven by the elevated P_b/P_f in that subgroup (Figure 2, panel B).

Being a global wave reflection coefficient, P_b/P_f integrates all factors affecting wave reflection. Given the absence of any significant correlation between P_b/P_f and Γ, it is to be concluded that local Γ along the aorta contributes little to the total wave reflection. Nevertheless, it cannot be excluded that local reflections arising from impedance mismatch between the aorta and the arteries branching off the aorta play a role. Given the fact that the impact of MFS on biomechanical properties of blood vessels is mainly confined to the proximal aorta which is subject to more rapid ageing, impedance differences would be most important in young subjects, what would fit with the fact that P_b/P_f was most elevated in the youngest subjects.

Table 2. Correlation between global and local wave reflection (MFS + CTRL). Significant correlations are displayed in italic; *: P<0.05; **: P<0.01.

	AIx	**P_b/P_f**	**$\Gamma_{AA\text{-}DA}$**	**$\Gamma_{DA\text{-}DIA}$**	**$\Gamma_{DIA\text{-}AB}$**
AIx	-	*0.463***	-0.214	-0.245	*0.292**
P_b/P_f	*0.463***	-	-0.025	-0.097	0.137
$\Gamma_{AA\text{-}DA}$	-0.214	-0.025	-	-0.060	-0.217
$\Gamma_{DA\text{-}DIA}$	-0.245	-0.097	-0.060	-	-0.055
$\Gamma_{DIA\text{-}AB}$	*0.292**	0.137	-0.217	-0.055	-

Finally, some methodological consideration should be formulated. (i) We scaled carotid diameter distension waveforms to assess carotid systolic pressure and pulse pressure. Although this methodology was found to be adequate [9], the relation between diameter and pressure is nonlinear [20], and we may have underestimated carotid systolic and pulse pressure, especially in the older subjects or in subjects with high blood pressure. (ii) The MFS and CTRL group were not matched for body size. It was an option to match the control population also in length, but we choose to take a sample of the general, healthy population (rather than a subpopulation of tall healthy subjects) and to compensate for body length via covariant analysis. (iii) For the calculation of local reflection coefficients (via formulas 3 and 4), carotid pressure was assumed to adequately represent pressure along the aorta. (iv) By inclusion of older Marfan patients, it cannot be excluded that the population is biased in the sense that older patients would have a 'milder' manifestation of the

ISSN: 1727-1983

disease, as they have reached a higher age without surgery despite the presence of the disease.

Conclusions

We conclude that (i) Marfan disease affects the normal pattern of evolution of characteristic impedance along the aorta, and hence leads to changes in local aortic reflection properties; (ii) Wave reflection, as quantified by global parameters such as the augmentation index or the backward-to-forward pressure wave ratio, is elevated in Marfan disease, especially in the young; (iii) the exact contribution of local reflections to the global effect of wave reflection remains to be determined.

Acknowledgements

This study was supported by a research grant from the Ghent University (BOF 011D4701) (J. De Backer) and by a research grant from the Fund For Scientific Research Belgium (FWO G029002) (A. De Paepe). Johan De Sutter is a senior clinical investigator of the Fund for Scientific Research – Flanders (Belgium) (FWO – Vlaanderen).

References

[1] DE PAEPE, A., DEVEREUX, R. B., DIETZ, H. C., HENNEKAM, R. C.PYERITZ, R. E. (1996). Revised diagnostic criteria for the Marfan syndrome. *Am J Med Genet* **62,** 417-426.

[2] PYERITZ, R. E.MCKUSICK, V. A. (1979). The Marfan syndrome: diagnosis and management. *N Engl J Med* **300,** 772-777.

[3] HIRATA, K., TRIPOSKIADIS, F., SPARKS, E., BOWEN, J., WOOLEY, C. F.BOUDOULAS, H. (1991). The Marfan syndrome: abnormal aortic elastic properties. *J Am Coll Cardiol* **18,** 57-63.

[4] JEREMY, R. W., HUANG, H., HWA, J., MCCARRON, H., HUGHES, C. F.RICHARDS, J. G. (1994). Relation between age, arterial distensibility, and aortic dilatation in the Marfan syndrome. *Am J Cardiol* **74,** 369-373.

[5] O'ROURKE, M. F. (1999). Mechanical principles. Arterial stiffness and wave reflection. *Pathol Biol (Paris)* **47,** 623-633.

[6] GROENINK, M., DE ROOS, A., MULDER, B. J., SPAAN, J. A.VAN DER WALL, E. E. (1998). Changes in aortic distensibility and pulse wave velocity assessed with magnetic resonance imaging following beta-blocker therapy in the Marfan syndrome. *Am J Cardiol* **82,** 203-208.

[7] GROENINK, M., DE ROOS, A., MULDER, B. J., VERBEETEN, B., JR., TIMMERMANS, J., ZWINDERMAN, A. H., SPAAN, J. A.VAN DER WALL, E. E. (2001). Biophysical properties of the normal-sized aorta in patients with Marfan syndrome: evaluation with MR flow mapping. *Radiology* **219,** 535-540.

[8] SEGERS, P., RABBEN, S. I., DE BACKER, J., DE SUTTER, J., GILLEBERT, T. C., VAN BORTEL, L.VERDONCK, P. (2004). Functional analysis of the common carotid artery: relative distension differences over the vessel wall measured in vivo. *J Hypertens* **22,** 973-981.

[9] VAN BORTEL, L. M., BALKESTEIN, E. J., VAN DER HEIJDEN-SPEK, J. J., VANMOLKOT, F. H., STAESSEN, J. A., KRAGTEN, J. A., VREDEVELD, J. W., SAFAR, M. E., STRUIJKER BOUDIER, H. A.HOEKS, A. P. (2001). Non-invasive assessment of local arterial pulse pressure: comparison of applanation tonometry and echo-tracking. *J Hypertens* **19,** 1037-1044.

[10] VERBEKE, F., SEGERS, P., HEIREMAN, S., VANHOLDER, R., VERDONCK, P.VAN BORTEL, L. M. (2005). Noninvasive Assessment of Local Pulse Pressure: Importance of Brachial-to-Radial Pressure Amplification. *Hypertension* **46,** 244-248. Epub 2005 May 2023.

[11] O'ROURKE, M. F., AVOLIO, A.QASEM, A. (2003). Clinical assessment of wave reflection. *Hypertension* **42,** e15-16; author reply e15-16. Epub 2003 Sep 2022.

[12] MURGO, J. P., WESTERHOF, N., GIOLMA, J. P.ALTOBELLI, S. A. (1980). Aortic input impedance in normal man: relationship to pressure wave forms. *Circulation* **62,** 105-116.

[13] WESTERHOF, N., SIPKEMA, P., VAN DEN BOS, C. G.ELZINGA, G. (1972). Forward and backward waves in the arterial system. *Cardiovascular Research* **6,** 648-656.

[14] MILNOR, W. R. (1989). *Hemodynamics*. Williams&Wilkins, Baltimore, Maryland, USA.

[15] NICHOLS, W.O'ROURKE, M. (1998). *McDonald's Blood Flow in Arteries*. Edward Arnold, London.

[16] SEGERS, P.VERDONCK, P. (2000). Role of tapering in aortic wave reflection: hydraulic and mathematical model study. *J Biomech* **33,** 299-306.

[17] TING, C. T., CHANG, M. S., WANG, S. P., CHIANG, B. N.YIN, F. C. (1990). Regional pulse wave velocities in hypertensive and normotensive humans. *Cardiovasc Res* **24,** 865-872.

[18] GILLESSEN, T., GILLESSEN, F., SIEBERTH, H., HANRATH, P.HEINTZ, B. (1995). Age-related changes in the elastic properties of the aortic tree in normotensive patients: investigation by intravascular ultrasound. *Eur J Med Res* **1,** 144-148.

[19] YIN, F. C., BRIN, K. P., TING, C. T.PYERITZ, R. E. (1989). Arterial hemodynamic indexes in Marfan's syndrome. *Circulation* **79,** 854-862.

[20] MEINDERS, J. M.HOEKS, A. P. (2004). Simultaneous assessment of diameter and pressure waveforms in the carotid artery. *Ultrasound Med Biol* **30,** 147-154.

ISSN: 1727-1983